

A New Way to Integrate GPS and INS Wavelet Multiresolution Analysis

Naser El-Sheimy, Ahmed Osman, Sameh Nassar, and Aboelmagd Noureldin

What do fingerprints, Brahms Hungarian Dance Number 1, El Niño, and GPS have in common? They are all being subjected to the relatively new mathematical technique known as *wavelet analysis*.

Wavelet analysis is an extension of Fourier analysis, the classical technique that decomposes a signal into its frequency components. However, Fourier analysis cannot determine the exact time at which a particular frequency occurred in the signal. Wavelet analysis, on the other hand, allows scientists and engineers to study the frequency structure of time-varying signals with unprecedented time resolution. In fact, a signal can be decomposed to obtain a time history of the different frequency bands making up the signal — an approach termed *multiresolution analysis*. Wavelet analysis can also compress data for more efficient storage and transmission, replacing the original data values with far fewer wavelet transform coefficients.

Although the roots of wavelet analysis can be traced back to the 1930s, the development of the technique for various applications in engineering and the sciences began only about 20 years ago. But in that relatively short time (on the history of mathematics timescale), the technique of wavelet analysis has been adopted for a huge variety of applications, from fingerprint compression to improved processing of GPS data.

- **Making Room for Fingerprints.** A digitized high-resolution fingerprint image requires about half a megabyte of storage, and a complete fingerprint card needs about 10 megabytes. While this might not seem like much, imagine the task of digitizing and stor-

ing the approximately 200 million fingerprint cards occupying an acre of filing cabinets at the U.S. Federal Bureau of Investigation in Washington, D.C. Using wavelet analysis, a digitized fingerprint card can be compressed by a factor of 15 or so, greatly easing the storage problem and allowing fingerprint images to be more quickly transmitted from one place to another.

- **Brahms Revisited.** Wavelet analysis has even been used to restore a heavily damaged recording of Brahms playing one of his own compositions. Part of Hungarian Dance Number 1 was recorded in 1889 on Thomas Edison's original wax-cylinder phonograph. Wavelet analysis of re-recordings of the original, despite being immersed in noise, has allowed researchers to discover that Brahms took liberties with his own published score. For example, he doubled the length of eighth notes in some places, shifted the emphasis on notes in others, and even improvised at times rather than follow the score. 

- **Enhancing GPS Accuracy.** Wavelet analysis is also being used to improve the accuracy of GPS. These uses include the de-noising of GPS pseudorange measurements, cycle-slip detection and elimination in GPS carrier-phase measurements, and separating biases such as multipath from high-frequency receiver noise. Wavelet analysis can also determine anomalies in GPS data used for deformation analysis and to remove seasonal variations and noise from a GPS time series to better estimate crustal motion.

In this month's column, University of Calgary researchers discuss the use of wavelet analysis to improve the integration of differential GPS with an inertial navigation system. —R.B.L.

Most present-day vehicular positioning systems depend on Kalman filtering to integrate inertial navigation system (INS) and GPS or differential GPS (DGPS) outputs. Although widely used, the Kalman filtering-based estimation procedure has some drawbacks related to computation load, immunity to noise effects, and observability. This article suggests a new methodology based on wavelet transformation for INS/DGPS integration. In addition, it offers a technique to improve the stand-alone INS positioning accuracy during GPS signal blockages. The new proposed method is based on separately processing the INS and the DGPS navigation parameter outputs with multilevel wavelet

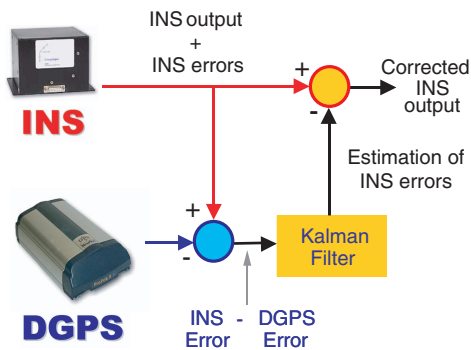
decomposition. The DGPS decomposition is compared with the corresponding INS decomposition. The differences are used to reconstruct the navigation parameter error signal, which is then used to correct the INS navigation output. The results have shown that substantial improvement in INS/DGPS accuracy could be obtained by applying wavelet multiresolution analysis.

Present-day vehicle navigation systems rely on GPS as the main positioning system. However, GPS can provide this type of information only when there is a direct line of sight to at least four satellites. In other words, the system does not work well in urban areas because of signal blockage and attenuation, which deteriorate the positioning accuracy. So in such environments

one cannot depend on GPS as a stand-alone system.

Furthermore, if the vehicle system is supplied with measurements or corrections from a reference station via a radio link of some kind (differential GPS or DGPS), the link also must be maintained or reduced positioning accuracy will result. More recently, and accepting that these techniques must inevitably cost more than GPS as a stand-alone system, the concept of combining complimentary navigation systems such as an INS has been used with commercial applications.

The objective of INS/DGPS integration is the fusion of all available data from various sensors to obtain an optimal navigation solution. Traditionally, a Kalman filter com-



▲ **FIGURE 1** An inertial navigation system (INS) and a GPS receiver that acquires differential corrections (DGPS) can be integrated into a single system using Kalman filtering.

bines data from the sensors, which may contain different sources of errors. Figure 1 shows a simplified scheme of the Kalman filter process.

In an integrated system, the INS outputs are compared with the outputs of the DGPS. Errors between the two are subjected to Kalman filtering, which is set to approximate the state model of the various positioning errors. (The state model describes how a platform being navigated changes its state — that is, its position, velocity, and attitude — from epoch to epoch.) The Kalman filter determines optimal estimates of the errors associated with the INS outputs in real time. Kalman filtering enhances the performance of the navigation system by removing the effect of these errors during the continuous navigation process. As shown in Figure 1, the errors estimated by the Kalman filter are removed from the INS outputs to provide corrected inertial output in a closed-loop fashion.

Although the Kalman filter represents one of the best solutions for INS/DGPS integration, it still has some drawbacks. It only works well under certain predefined models, for example. If the filter is exposed to input data that do not fit the model, it will not provide reliable estimates.

Another problem related to the Kalman filter is the observability of the different states. A system is considered to be nonobservable if one or more state variables are hidden from the view of the observer (that is, the measurements). If the unobserved process is not stable, the corresponding es-

timations will be similarly unstable. For example, when the error state equation of an INS is examined, one can determine an azimuth error state that is weakly coupled with the velocity error states. Therefore, optimal estimates of the velocity errors provided by the Kalman filter due to GPS position or velocity updates will not benefit the azimuth accuracy. Thus, the azimuth error state is a weakly observable component. Furthermore, during GPS outages, Kalman filtering provides poor prediction of stand-alone INS.

This article describes a new multisensor integration method that uses wavelet multi-resolution analysis and evaluates the proposed architecture using field-test data.

The proposed method is based on separately processing the INS and the DGPS navigation parameter outputs with multi-level wavelet decomposition. This technique decomposes a signal into two components (approximation and details) at a sequence of resolutions. The DGPS approximation and the details of the navigation output are compared with the corresponding INS approximation and details. The errors between the two are used to reconstruct the navigation parameter error signal, which is used to correct the INS navigation output.

Multiresolution Analysis

By analyzing INS or DGPS output signals in the frequency domain, one can see that these signals are composed of several frequency components. For many signals, frequency domain analysis using the Fourier transform (FT) is extremely useful because the signal's frequency content is of great importance for understanding the nature of the signal and any noise that contaminates it. However, Fourier analysis has a serious drawback: Transforming to the frequency domain causes time information to be lost. When looking at a Fourier transform of a signal, it is impossible to tell when a particular event took place.

In an effort to overcome this deficiency, the same transform was adapted to analyze only a small window of the signal at a time. This technique, presently known as the *short-*

time Fourier transform (STFT), maps a signal into a two-dimensional function of time and frequency. STFT's only drawback is that once the user chooses a particular size for the time window, that window is the same for all frequencies. Many signals require a more flexible approach (for example, one in which the window size is varied to determine more accurately either time or frequency).

Wavelet analysis represents the next logical step, which is based on a windowing technique with variable-sized regions. The wavelet transform (WT) allows the use of long time intervals for more-precise low-frequency information and shorter regions for high-frequency information. In general, the major advantage of wavelets is the ability to perform local analysis — that is, to analyze a localized area of a larger signal.

Wavelet Transform. The WT of a continuous (analog) signal $x(t)$ is known as the *continuous wavelet transform* (CWT) and is defined as

$$CWT(a,b) = \frac{1}{\sqrt{a}} \int_{-\infty}^{\infty} x(t) \psi\left(\frac{t-b}{a}\right) dt \quad (1)$$

in which a is the scaling parameter and b is the time-shift parameter (discussed later in this article). The signal $x(t)$ is transformed by an analyzing function $\psi((t-b)/a)$. The analyzing function $\psi(t)$ is not limited to the complex exponential as used in the Fourier transform. In fact, the only restriction on $\psi(t)$ is that it must be short and oscillatory; that is, it must have a zero mean and decay quickly at both ends. This restriction ensures that the integral in Equation 1 is finite and gives the name *wavelet* or “small wave” to the transform.

Figure 2 gives examples of two wavelets showing their oscillatory and potentially nonsinusoidal nature. If we define a wavelet with $a = 1$ and $b = 0$, we have a *basis* or *mother wavelet*. The mother wavelet can be scaled (dilated) and shifted (translated) to produce *daughter wavelets*.

According to the definition of the inner product, the CWT can be thought of as the inner product of the original signal with scaled, shifted versions of the basis wavelet function $\psi(t)$

$$CWT(a,b) = \int x(t) \bullet \psi(t) dt = \langle f, \psi_{a,b} \rangle \quad (2)$$

in which



▲ FIGURE 2 Wavelets ("small waves") must be short and oscillatory, with zero mean. They mimic the variations in real signals. The two wavelets pictured here are examples of Daubechies wavelets.

$$\psi_{a,b} = \frac{1}{\sqrt{a}} \psi\left(\frac{t-b}{a}\right) \quad (3)$$

and in which a represents the scale, which determines the oscillating behavior of the particular daughter wavelet, and b represents the shifting of the mother wavelet, which is important for this transform to provide time-localization information of the original signal. The angled brackets are a short-form notation for the time average.

For ease of computer implementation, the discrete wavelet transform (DWT) is used. The scaling and shifting variables are discretized so that wavelet coefficients can be described by two integers, m and n . Thus, the DWT is given as

$$DWT(m,n) = \frac{1}{\sqrt{a_0^m}} \sum_k x[k] \psi[a_0^{-m} n - k] \quad (4)$$

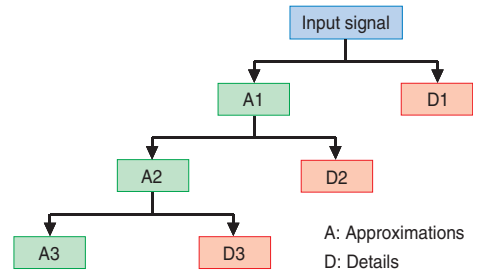
in which $x[k]$ is a digital signal or a digitized version of an analog signal with sample index k , and $\psi(n)$ is the mother wavelet. With different choices of m , we obtain a geometric scaling: $1, 1/a_0, 1/a_0^2, \dots$. This scaling gives the DWT logarithmic frequency coverage in contrast to the uniform frequency coverage of the STFT. It is found in practice that the most convenient value of a_0 is 2. This analysis method then consists of decomposing a signal into components at several frequency levels that are related by powers of two (a dyadic scale).

Wavelet Multiresolution Analysis. Multiresolution analysis (MRA) determines the general WT. It allows the decomposition of signals into various resolution levels. The data with coarse resolution contain information about lower-frequency components and retain the main features of the original signal. The data with finer resolution retain information about the higher-frequency components. The filtering approach to multiresolution WT is to form a series of

half-band filters that divide a spectrum into a high-frequency band and a low-frequency band. It is formulated on a scaling function or *low-pass filter* (LP) and a wavelet function or *high-pass filter* (HP). MRA builds a pyramidal structure that requires an iterative application of scaling and wavelet functions to low-pass and high-pass filters, respectively. These filters initially act on the entire signal band at the high frequencies (small-scale) first and gradually reduce the signal band at each stage. As in **Figure 3**, the high-frequency band outputs are represented by the detail coefficients (D1, D2, D3), and the low-frequency band outputs are represented by the approximation coefficients (A1, A2, A3).

Implementation of DWT. The multiresolution filter bank shown in **Figure 3** implements the DWT using the LP and HP wavelet filter coefficients to decompose an input signal into different frequency levels. For example, if the original input signal is being sampled at f_s Hz, then the highest frequency that the sampled signal would faithfully represent is $f_s/2$ (based on the Nyquist theorem). This is seen as the output of the HP filter, which is the first detail, D1, in **Figure 3**. In other words, the first detail would capture the band of frequencies between $f_s/2$ and $f_s/4$. Likewise, the second detail would capture the band of frequencies between $f_s/4$ and $f_s/8$, and so on.

Digital signal processing uses exclusively orthogonal wavelets to separate effectively the low- and high-frequency signal contents at each resolution level. The nonredundant representation and perfect reconstruction of the original signal can be realized only through compactly supported wavelets. Unlike the continuous wavelet transform, the discrete wavelet transform is supported by two filters, low pass and high pass, which have a certain number of coefficients that can effectively separate the low-pass and the high-pass frequencies of the signal. The wavelets that are frequently used for signal processing are Daubechies (named after their discoverer, Ingrid Daubechies), bi-orthogonal (involving two sets of low- and high-pass filters), coiflets (variations on Daubechies' wavelets), and symlets (nearly symmetrical wavelets also proposed by



▲ FIGURE 3 The wavelet decomposition tree. At each level in the wavelet decomposition procedure, the signal is split between the low-frequency approximation and the high-frequency details.

Daubechies). These wavelets exhibit different attributes and performance criteria when applied to specific applications such as detecting signal transients, signal compression, and de-noising.

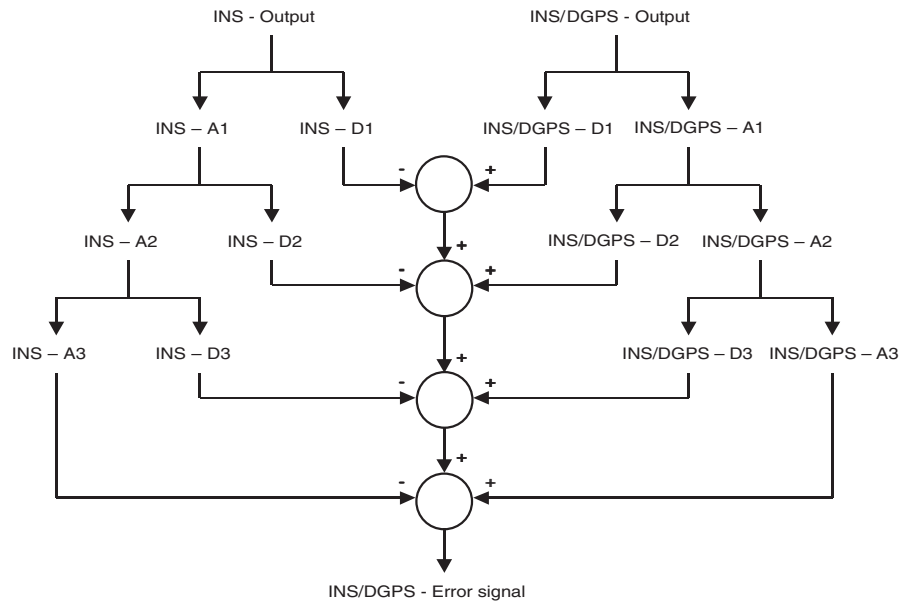
Choosing an appropriate wavelet filter is important in identifying the characteristics of transient analysis. Because the convolution sum between the signal and the wavelet-system filters measures the similarity between the signal and the wavelet basis function, the simplest method for choosing a wavelet to observe the signal's time-frequency behavior is to copy the form of the transient signal. However, most transient signals, which are exponentially damped sinusoids, cannot be wavelet basis functions because of their nonzero mean.

INS/DGPS Integration

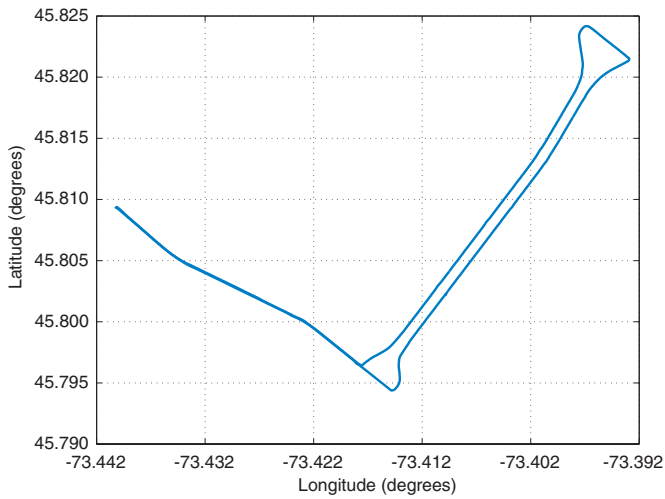
The accelerometers and gyroscopes in an INS measure linear acceleration and angular orientation rates very accurately and with minimum time delay. For short time intervals, the integration of acceleration and angular rate results in extremely accurate velocity, position, and attitude determinations, with almost no noise or latency (time lag). However, because the INS outputs are obtained by integration of accelerations and the measurements contain residual bias errors of both the accelerometers and the gyroscopes, they drift with time, giving rise to low-frequency errors. To obtain accurate outputs at all frequencies, the INS should be updated periodically using external measurements. GPS- (or preferably, the more accurate DGPS-) derived velocities and positions can provide such updates and ideally complement the INS output.

We implemented the MRA technique to determine the differences between the INS and DGPS position outputs after having compared the corresponding velocity and position components at several wavelet decomposition levels. These differences represent, in general, the INS errors and are used to correct the INS outputs during brief GPS outages. Whenever the GPS signal is available, the error signal for each navigation parameter is estimated. A polynomial is fitted to each INS error signal to model its variation with time. Then, when a GPS outage occurs, the error model of each navigation parameter predicts the deviation in the INS output and compensates for it. The block diagram shown in **Figure 4** provides an overview of our MRA INS/DGPS integration procedure.

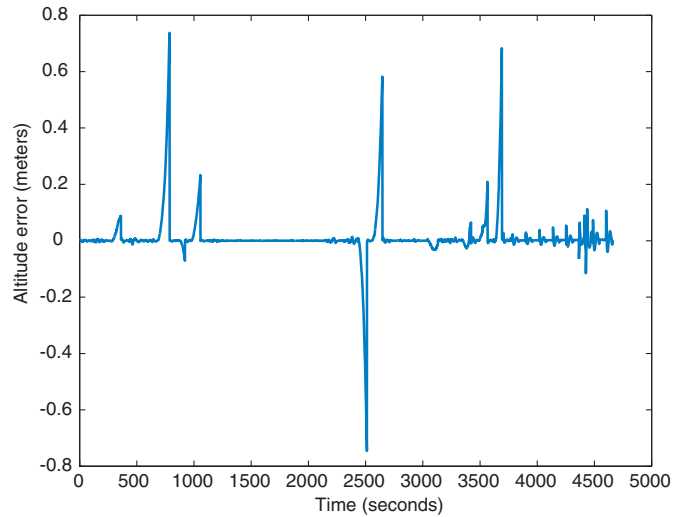
Error Signal Estimation. One can estimate the differences between the INS and the DGPS navigation parameter values (the INS error) by using the theory of wavelet MRA.



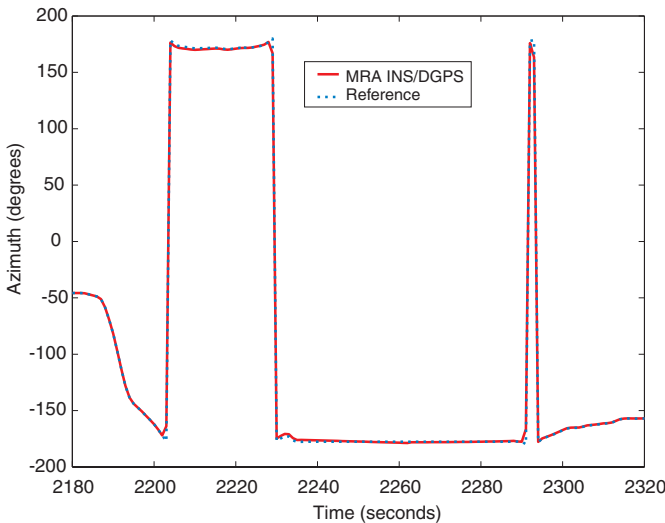
▲ **FIGURE 4** In the INS/DGPS integration scheme using wavelet multiresolution analysis, the INS/DGPS output is combined with the INS output at each resolution level to determine the overall INS/DGPS error signal.



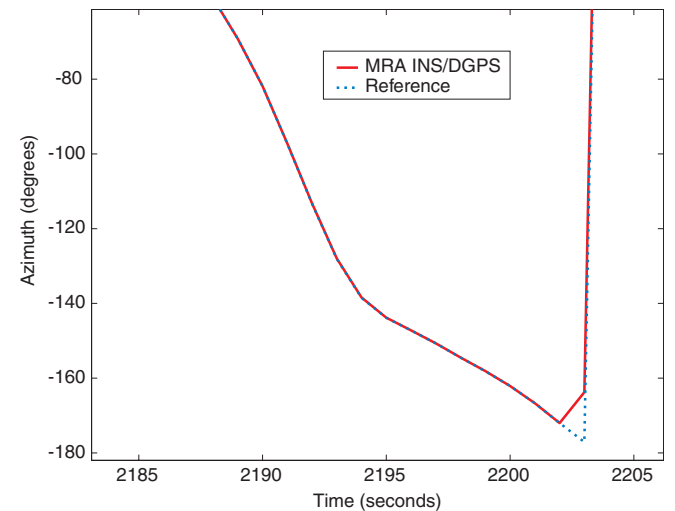
▲ **FIGURE 5** To test the INS/DGPS integration scheme, kinematic measurements were obtained using a van following the illustrated trajectory.



▲ **FIGURE 6** The altitude errors using the INS/DGPS multiresolution analysis method were close to zero when GPS signals were available, growing to a maximum value of ± 0.8 meters during simulated GPS outages.



▲ **FIGURE 7** When GPS signals were available, the azimuth of the van trajectory determined using the multiresolution analysis technique matched the reference solution obtained using a standard Kalman filter approach except at sharp turns.



▲ **FIGURE 8** At sharp turns, the multiresolution analysis technique performed better than the reference Kalman filter approach by virtue of its ability to more faithfully follow the high-frequency variation of the turns.

Both INS and DGPS outputs are split into three decomposition levels using a wavelet transform. After extensive studies, we selected a Daubechies 4 (db4) wavelet to be the analyzing mother wavelet. A db4 has eight filter coefficients in its HP and LP filters. We used a sliding data window with a fixed size of one minute (consisting of 60 one-second samples) in this analysis. A *slid-*

ing data window means that when a new sample enters the window, the oldest one is discarded. For each new sample entering the data window, the analyzing software performs a series of calculations summarized in Equations 5 through 7.

In the wavelet domain, using the DWT, the wavelet coefficients that represent each of the INS navigation parameters in the

three decomposition levels are

$$C_{INS} = [cA_{i1} | cD_{i1} | cA_{i2} | cD_{i2} | cA_{i3} | cD_{i3} |] \quad (5)$$

and each DGPS parameter can be represented as

$$C_{GPS} = [cA_{g1} | cD_{g1} | cA_{g2} | cD_{g2} | cA_{g3} | cD_{g3} |] \quad (6)$$

By subtracting the wavelet coefficients of each of the DGPS outputs from the corre-

sponding wavelet coefficients of each of the INS outputs, the wavelet coefficients of the error signals can be extracted as

$$E = [|cA_{e1} |cD_{e1} |cA_{e2} |cD_{e2} |cA_{e3} |cD_{e3} |] \quad (7)$$

The error signal can then be reconstructed from the wavelet coefficients obtained in Equation 7. The error signal can be smoothed by neglecting the highest frequency band (the band reconstructed from the detail coefficients) from the reconstructed signal. This band contains the distortions in the position and the attitude components. The analyzing software then fits a third-order polynomial to the estimated error signal for all the data points in the data window. This polynomial predicts the error signal during a GPS signal blockage. Once a GPS signal blockage is detected, the error signal is estimated for each new sample and then is subtracted from the navigation parameter signal to get the corrected value for that parameter at the epoch of the new sam-

ple. The error signal estimation is continued using the fitted polynomial technique until the GPS signals are reacquired and the overall procedure is repeated.

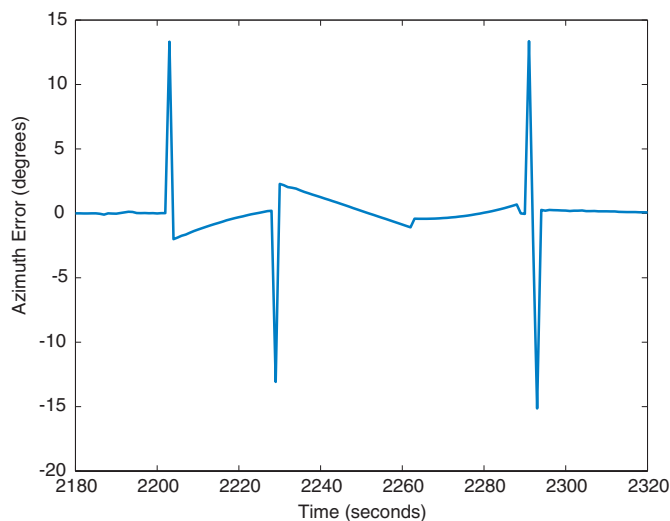
Adaptive Error Correction. We have developed an adaptive technique for predicting the error signal from the fitted polynomial during the outage of the GPS signals. This technique is based on using the error-fitted polynomial of the last data window before the GPS outage. Immediately, at the moment following the GPS outage, the polynomial obtained from the last data window estimates the error signal at this epoch, and the navigation parameter is corrected. Consequently, a new error signal with the same window length (one minute) is established by discarding the oldest (that is, the first) sample in the previous data window and by inserting the estimated one as the last sample in the data window. This new error data window fits a new polynomial that estimates the error signal at the next epoch and

consequently corrects the navigation parameter. This process is repeated until the GPS signals are reacquired.

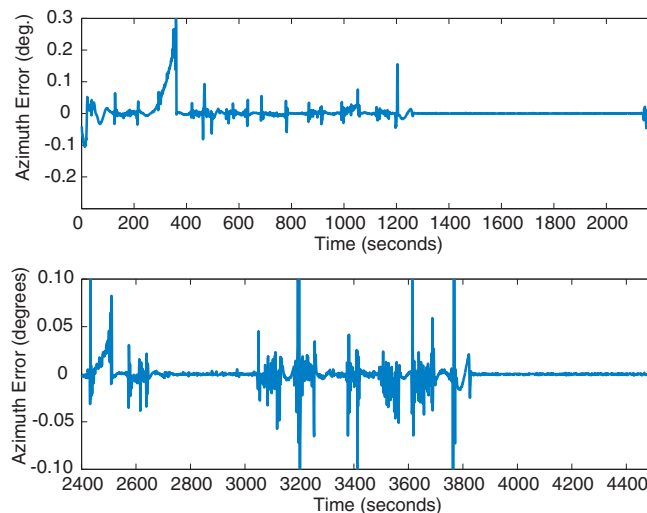
Using an adaptive error data window with newly fitted polynomials enhances the accuracy of the estimated error signal considerably. This occurs mainly because the newly estimated samples depend on a real and accurate error signal that was obtained before the outage of the GPS signals.

Results and Discussion

We collected the kinematic data used in the analysis in Laval, Québec, Canada, with the Video-Inertial-Satellite (VISAT) Van mobile mapping system. The VISAT system integrates a cluster of video cameras, an INS, and GPS receivers. The DGPS position and velocity control the INS error propagation, and the high-frequency INS positions bridge GPS outages, correct cycle slips, and give precise interpolation between GPS updates. The updated INS/DGPS information is



▲ **FIGURE 9** The azimuth differences between the multiresolution analysis technique and standard Kalman filtering were as large as 15 degrees at sharp turns.



▲ **FIGURE 10** During simulated GPS outages of up to 100 seconds, the multiresolution analysis technique provided azimuths with errors of less than 0.3 degrees.

used to geometrically correct the images collected by the video cameras which are used, in postmission, for mapping and GIS applications. In this test, we used two geodetic-grade dual-frequency GPS receivers (for postmission-processed DGPS) and a navigation-grade INS. The minimum number of available satellites was seven, and the average position dilution of precision was 1.5. The average van speed was 50 kilometers per hour with a maximum reference-rover receiver distance of four kilometers. **Figure 5** illustrates the trajectory of this test.

To investigate the performance of our proposed MRA INS/DGPS integration method, we processed the van data twice—the first time in an INS/DGPS integration mode with conventional Kalman filtering to obtain a reference solution and the second time in INS/DGPS integration mode with some simulated GPS outage periods. To obtain positioning errors accumulated during the selected outage periods, we subtracted the reference solution from the solution that contains these outages. Because GPS signals were always actually available during the test, the initial INS/DGPS integrated solution can be considered as an accurate reference with which to compare the results from the simulated outages. We simulated a total of 10 GPS outages (outage intervals ranged from 75 to 100 seconds), all while the van was in motion.

We applied the proposed wavelet MRA method described in the previous section to the position and velocity components representing the motion of the vehicle. We compared each position and velocity component estimated from the INS, in free navigation mode (that is, uncorrected by DGPS), with the corresponding DGPS component as shown in **Figure 4** and then computed the error signal. Next we compared the results of the MRA INS/DGPS method to the reference solution. In addition, to investigate the applicability of the proposed MRA method on the attitude components, we applied the scheme shown in **Figure 4** to the INS and the INS/DGPS attitude components.

Figure 6 shows the altitude error (δh) during 78 minutes of the kinematic test. The figure clearly shows that δh was almost zero throughout the entire time the GPS signals were available, and an error of less than 0.8 meters was accumulated at the end of each GPS outage. We have obtained similar results for both the latitude and the longitude position components.

We noted that while GPS signals were available, the azimuth solutions of the MRA method were almost the same as the reference values except at sharp turns as shown in **Figure 7**, where the vehicle reverses its direction.

At one of these sharp turns (see **Figure 8**),

the MRA solution responded faster than did the INS/DGPS reference solution, providing accurate monitoring of the vehicle's azimuth. This faster response of the MRA method results from its inclusion of the high-frequency components (where sharp turns appear) in its details. On the other hand, the INS/DGPS reference integration is implemented by a Kalman filter, which is an LP filter and cannot detect such high-frequency components. Therefore, the largest differences between the two solutions took place at the sharp turns, as **Figure 9** illustrates. Although the differences between the two solutions are relatively high (10–15 degrees), they occur almost instantaneously during the test and do not affect the overall system accuracy.

During the simulated GPS outages, the MRA method provided the azimuth with errors of less than 0.3 degrees for GPS signal blockages lasting less than 100 seconds. **Figure 10** shows the azimuth errors for portions of the van trajectory in which there are no sharp turns. The upper and the lower plots show, respectively, the azimuth error for the first 2000 seconds and for the last 2000 seconds of the test. It can be noticed in both figures that the azimuth errors were kept to less than 0.3 degrees. Better accuracy levels (errors less than 0.05 degrees) were obtained for the other attitude components (pitch and roll).

Conclusion

The suggested wavelet MRA INS/DGPS method offers a new technique for removing INS errors in real time. A model of INS errors determined at the MRA data-processing stage is used to compensate for the INS outputs during GPS signal blockage. Experimental results demonstrated the advantages of the new approach in terms of performance and computational efficiency.

Analysis of the results showed that the increase of errors for some of the navigation components may be related to the improper modeling of INS errors as polynomials. We plan to improve the method by means of an artificial neural network technique that will allow us to more accurately model and predict INS errors during GPS outages.

Acknowledgments

The study reported in this article was supported in part through grants from the Natural Sciences and Engineering Research Council of Canada and the Geomatics for Informed Decisions Network of Centres of Excellence. This article is based on the paper *INS/DGPS Integration Utilizing Wavelet Multi-Resolution Analysis* presented at The Institute of Navigation's National Technical Meeting held in Anaheim, California, January 22–24, 2003. 🌐

Manufacturers

Data were provided by **Thales Navigation** (Santa Clara, California) *Ashtech Z12* GPS receivers and a **Honeywell International Inc.** (Morristown, New Jersey) *Laseref III* navigation-grade INS.

Naser El-Sheimy is an associate professor and interim head of the Department of Geomatics Engineering at The University of Calgary (U. of C.) in Calgary, Alberta, Canada. He holds the Canada Research Chair (CRC) in Mobile Multisensors Geomatics Systems, and he is the team leader of the multisensor research group at the University of Calgary. His area of expertise is the integration of INS/GPS and imaging sensors for mapping and GIS applications, with special emphasis on the use of multisensors in mobile mapping systems. He is the chairman of the International Association of Geodesy working group on mobile multisensor systems and the chairman of the International Federation of Surveyors working group on kinematic and integrated positioning systems.

Further Reading

For a simplified introduction to wavelets, see

The World According to Wavelets: The Story of a Mathematical Technique in the Making, by B. Burke Hubbard, published by A.K. Peters, Ltd., Wellesley, MA, 1996.

For a more in-depth introduction, with an appendix of MatLab programs, see

Introduction to Wavelets and Wavelet Transforms: A Primer, by C.S. Burrus, R.A. Gopinath, and H. Guo, published by Prentice Hall, Englewood Cliffs, NJ, 1998.

For a discussion of the fast wavelet transform, see

"The Fast Wavelet Transform: Beyond Fourier Transforms" by M.A. Cody in *Dr. Dobb's Journal*, April 1992, pp. 16–28. An on-line version is available: <<http://www.ddj.com/documents/s=1722/ddj9204a/>>.

For an on-line Java-enabled wavelet tutorial, including multiresolution analysis, see

"Digital Signal Processing at Rice University: Java Wavelet Demo," <<http://www.dsp.rice.edu/software/EDU/>>.

For an on-line digest of articles about wavelets as well as lists of wavelet books, tutorials, introductions, and software, see

The Wavelet Digest, <http://www.wavelet.org/>>.

For a thorough discussion of signal errors and the mathematical techniques for analyzing them, see

Introduction to Random Signals, by R.G. Brown and P.Y.C. Hwang, published by John Wiley & Sons, Inc., New York, 1992.

For an introduction to the Kalman filter, see

"The Kalman Filter: Navigation's Integration Workhorse," by L.J. Levy in *GPS World*, Vol. 8, No. 9, September 1997, pp. 65–71.

For a discussion of inertial navigation system error handling with a Kalman filter, see

"Novel Kalman Filtering Method for the Suppression of Gyroscope Noise Effects in Pointing and Tracking Systems," by M.C. Algrain and D.E. Ehlers in *Journal of Optical Engineering*, Vol. 34, No. 10, 1995, pp. 3016–3030.

For further information about the VISAT Van, see

The Development of VISAT-A Mobile Survey System for GIS Applications, by N. El-Sheimy, a Ph.D. thesis published by the Department of Geomatics Engineering, The University of Calgary, Calgary, Alberta, Canada, UCGE Report No. 20101, 1996. An on-line version is available: <<http://www.geomatics.ucalgary.ca/Papers/Thesis/KPS/96.20101.NE/El-Sheimy.pdf>>.

Ahmed Osman is a Ph.D. candidate in the Department of Electrical and Computer Engineering at U. of C. He holds B.Sc. and M.Sc. degrees in electrical engineering from Helwan University, Cairo, Egypt. His research interest includes power system protection, digital signal processing, and wavelet multiresolution analysis.

Sameh Nassar is currently a Ph.D. candidate in the Department of Geomatics Engineering, U. of C. He holds a B.Sc. in surveying and geodesy and an M.Sc. in geomatics engineering, both degrees from Ain-Shams University, Cairo, Egypt. His research interests include positioning, navigation, and attitude determination using INS/GPS integration for georeferencing and airborne gravimetry.

Aboelmagd Noureldin is an assistant professor in the Department of Electrical and Computer Engineering at the Royal Military College of Canada in Kingston, Ontario, Canada. He holds a B.Sc. degree in electrical engineering and an M.Sc. degree in engineering physics from Cairo University, Giza, Egypt. In addition, he holds a Ph.D. degree in electrical engineering from U. of C. His research interests are related to inertial navigation and multisensor system integration.



"Innovation" is a regular column featuring discussions about recent advances in GPS technology and its applications as well as the fundamentals of GPS positioning. The column is coordinated by **Richard Langley**

of the Department of Geodesy and Geomatics Engineering at the University of New Brunswick, who appreciates receiving your comments and topic suggestions. To contact him, see the "Columnists" section on page 2 of this issue.